of 13%. The plastic limit for completely decomposed Norwood Tuff is 25%. In the Unified Soil Classification System these test results qualify the completely decomposed Norwood Tuff as lean clay.

Static conditions of the deformed Zigzag Sign landslide were modeled for dry conditions with Geostudio engineering software developed by Geo-Slope International, Ltd. The limit-equilibrium method built into Slope/W module was utilized to study the static slope stability. The model geometry was developed using a combination of seismic refraction, borehole, and dynamic cone penetration test data for the Zigzag sign landslide. Groundwater was not considered in the analysis, as the study was performed for dry slope conditions. Bedrock and slide mass material were the two regions modeled (Figure 3). The bedrock was considered impenetrable while the slide mass material was governed by the Mohr-Coulomb failure criterion. Material properties involved in modeling the slide mass included the unit weight of completely decomposed Norwood Tuff – 19.1 kN/m^3, the effective cohesion – 4.2 kPa, and the effective friction angle – 27° (Trandafir and Amini, 2009). Janbu's method was used to calculate the static safety factor along the sliding surface for the slope without a groundwater table within the slide mass (Janbu, 1954). The safety factor (*FS*) for the drained, deformed slope is 1.36, thus indicating a stable slope under dry, static conditions.

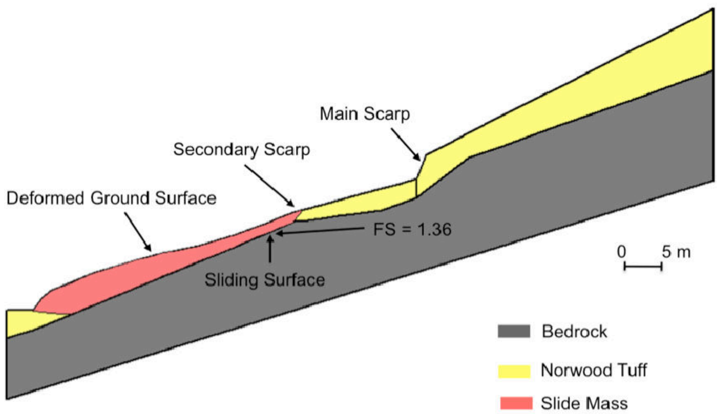

Figure 3. Static analysis of the Zigzag Sign landslide.

DYNAMIC DISPLACEMENT ANALYSIS OF ZIGZAG SIGN LANDSLIDE

A pseudo-static limit-equilibrium analysis with the Slope/W module was employed to determine the drained seismic yield coefficient using the same parameters as the static slope analysis. A trial-and-error approach was employed to adjust the magnitude of the horizontal seismic load acting on the landslide mass until a safety factor equal to one was achieved. The seismic coefficient associated with a safety factor of one represents the yield coefficient. Because the shear surface of the landslide was already known, the critical slip surface for each trial did not need to be determined. The analysis revealed a yield acceleration (i.e., yield coefficient multiplied by the gravitational acceleration) of 0.25*g* necessary to achieve a safety factor equal to one for the analyzed landslide in drained conditions.

Since no earthquakes have been yet recorded with modern instrumentation on the Weber Segment of the Wasatch Fault, example earthquakes from around the world were employed to simulate the seismic response of the Zigzag sign landslide. The parameters used to locate records with similar characteristics to the Weber Segment and the study area included normal faulting earthquakes with magnitudes M_0 ranging from 6.7 to 7.7, rupture distance ranging from 0 to 15 km, and rock site conditions with shear wave velocities ranging from 760 m/s to 1500 m/s. Six earthquake events were chosen and scaled to match as closely as possible the target spectrum acceleration. In addition, six seismic waveforms characterized by various Arias intensities were selected to correlate Arias intensity values with displacement and earthquake acceleration thresholds associated with large, potentially destructive landslide movements.

A Newmark sliding block analysis was employed to calculate permanent seismic displacements of the Zigzag Sign landslide (Newmark, 1965) under various horizontal input accelerograms. The finite-difference based numerical integration scheme characterizing the Newmark sliding block procedure was built into a computer code utilized in dynamic displacement calculations. Each acceleration-time history was scaled to various values of the peak earthquake acceleration within 0.1-1.0*g* using 0.1*g* increments. For each earthquake event the scaled peak acceleration coefficient (k_m) was plotted against the corresponding calculated permanent displacement (s_p) on a logarithmic scale (Figure 4). Such plot allows us to distinguish between peak earthquake accelerations associated with relatively small permanent displacements and peak earthquake acceleration values that may trigger large, potentially damaging slope movements. The intersection between the tangent to the asymptotic portion of the s_p-k_m curve and the horizontal axis provides the peak ground acceleration threshold (k_m^c, g) for earthquake-induced large, potentially damaging displacements. Peak acceleration values greater than this threshold may be considered unsafe due to an asymptotic increase in permanent seismic displacements with increasing k_m.

The relationship between the critical peak ground acceleration threshold and the amount of energy released by the earthquake was subsequently analyzed using normalized Arias intensities calculated for the positive and negative orientation of each seismic record. The normalized Arias intensity ($\bar{I}_A$) was calculated as follows:

$$\bar{I} = \frac{I_A}{\left(a_{\max}\right)^2}$$

where I_A represents the Arias intensity calculated for a specific earthquake accelerogram, *a(t)*, characterized by a peak earthquake acceleration $a_{\max} = k_m g$ and a duration t_s (i.e., $I_A = \frac{\pi}{2g}\int_0^{t_s} a^2(t)\, dt$).

For the analyzed input earthquakes, $\bar{I}_A$ varied from 1.83 to 63.15 s^3/m. The threshold peak earthquake acceleration coefficient to trigger large, potentially damaging dynamic landslide displacements ranged from 0.55 to 0.70*g* with an average value of 0.63*g* and a standard deviation equal to 0.04*g* (Figure 5).

CONCLUDING REMARKS

Results from the dynamic displacement analysis indicate that peak acceleration values greater than 0.55*g* should be considered unsafe for shallow landslides in completely decomposed Norwood Tuff due to an asymptotic increase in computed permanent displacement with increasing peak earthquake acceleration beyond this threshold. The analysis also revealed that the coefficient of peak ground acceleration threshold is not dependent on the normalized Arias Intensity of the seismic event.

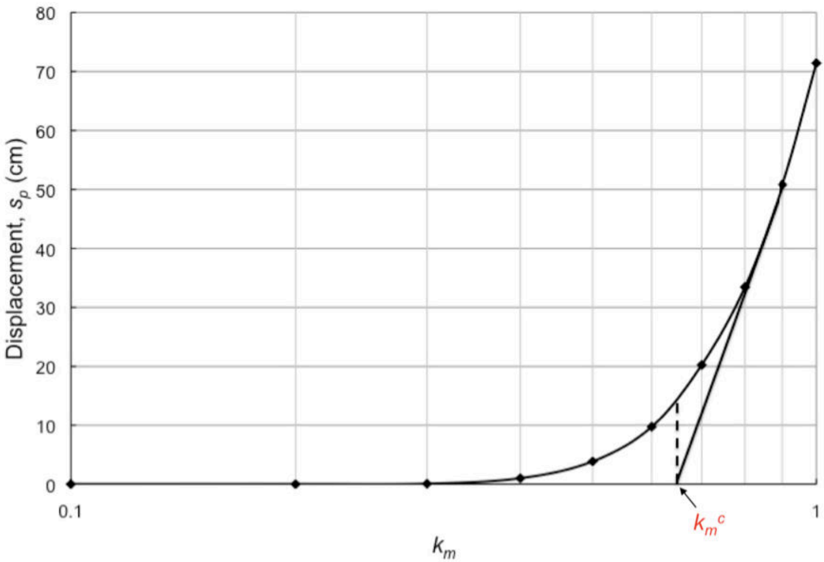

Figure 4. Typical relationship between peak earthquake acceleration coefficient (k_m^c) of a scaled seismic record and corresponding computed permanent landslide displacement (s_p).

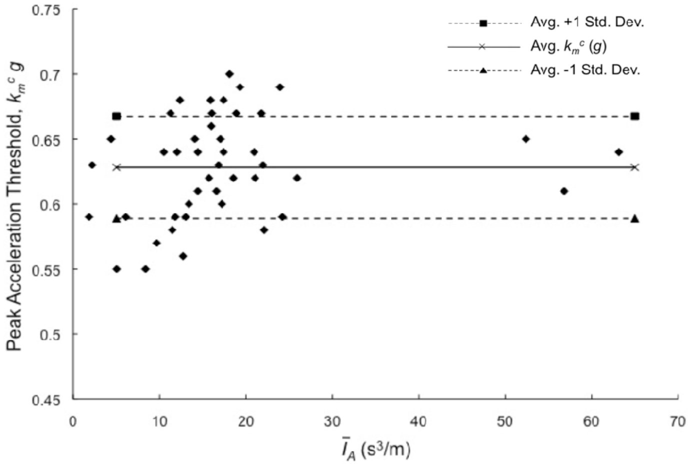

Figure 5. Relationship between the peak earthquake acceleration threshold and normalized Arias intensity.

REFERENCES

Ashland, F.X. (2007). Active landslides in the Creekside Drive area, Mountain Green, Morgan County, Utah, between June 2005 and December 2006. Utah Geological Survey Report of Investigation 260.

Ashland, F.X., Giraud, R.E., MDonald, G.N., and Elliott, A.H. (2008). Ground-water conditions in the Green Pond Landslide, Weber County, Utah. Utah Geological Survey Open-File Report 528.

Coogan, J.C. and King, J.K. (2006). Interim geologic map of the Durst Mountain quadrangle, Morgan and Weber Counties, Utah, Utah Geological Survey.

Duross, C.B., Personius, S.F., Crone, A.J., McDonald, G.N., and Lidke, D.J. (2009). Paleoseismic investigation of the northern Weber segment of the Wasatch Fault Zone at the Rice Creek trench site, North Ogden, Utah. Utah Geological Survey Special Study 130.

GEO-SLOPE International, Ltd. (2007). GeoStudio tutorials, Geo-Slope International Ltd, p 485.

Janbu, N. (1954). Applications of composite slip surfaces for stability analysis. In: Proceedings of the European conference on the stability of earth slopes, Vol. 3. Stockholm, pp. 39-43.

Newmark, N.M. (1965). Effects of earthquakes on dams and embankments. Geotechnique, Vol. 15 No. 2, pp. 139-149.

Stokes, W.L. (1977). Subdivisions of the major physiographic provinces in Utah. Utah Geol 4(1), pp. 1-17.

Trandafir, A.C. and Amini, Z.A. (2009) Yielding mechanism of shallow mass movements in completely decomposed Norwood Tuff: the Zigzag Sign landslide, Utah. Environmental Geology, Vol. 57, No. 6, pp. 1443-1451.

Intra- and Inter-Event Uncertainties of Ground Motion Attenuation Relations

Swagata Banerjee

Assistant Professor, Pennsylvania State University, University Park, PA 16802

Ground motion attenuation relationships have traditionally been used to describe the spatial distribution of earthquake ground motions. Attenuation models provide the ground motion intensities at different locations of the distribution region by combining two key estimates: (*i*) median values of ground motion intensities and (*ii*) aleatory uncertainty parameters namely inter- and intra-event uncertainty. The present study simulates inter- and intra-event uncertainties as Gaussian random variable and two-dimensional stationary Gaussian random field, respectively, assuming they are independent events. Earthquake records from Next Generation Attenuation or, NGA database are used for this purpose. Intensity of ground motions are measured in terms of peak ground acceleration (PGA). To use in the simulation process, nonlinear site response model is represented with a suitable probability distribution. Result shows that intra-event uncertainty is more significant than inter-event uncertainty.

INTRODUCTION

The empirical ground motion models (i.e., attenuation relationships) are in use over decades to describe the spatial distribution of earthquake ground motions. The functional form of attenuation relationships can generally be written as

$$\ln\left(Y_{ij}\right)=\ln\left(\hat{Y}_{ij}\right)+\eta_i+\varepsilon_{ij} \tag{1}$$

where Y_{ij} is the ground motion intensity (such as peak ground acceleration, or PGA) of i^{th} event at j^{th} station and $\hat{Y}_{ij}$ is the median ground motion intensity of the same event at that station. Y_{ij} is a recoded quantity while $\hat{Y}_{ij}$ represents the prediction from empirical attenuation equations. The most recent attenuation models known as Next Generation Attenuation or, NGA models provide the empirical equations for $\hat{Y}_{ij}$ (Abrahamson and Silva 2008, Campbell and Bozorgnia 2007, Boore and Atkinson 2008, Idriss 2007, and Chiou and Youngs 2008). η_i and ε_{ij} are two aleatory uncertainties respectively known as inter-event and intra-event uncertainty, and are introduced in the attenuation model to represent (collectively) the uncertainty associated with the predictive model. Inter-event uncertainty indicates the randomness of seismic events generated from a particular seismic source, while the intra-event uncertainty describes the random nature of a particular seismic event at different sites. Thus the random effect of ground motion distribution is incorporated in the empirical attenuation model. Median ground motion intensities in combination with these two aleatory uncertainties provide the expected intensities of ground motions at various sites in the neighboring region of earthquake epicenter.

Abrahamson and Silva (1992) performed regression analysis to calculate the effect of η_i and ε_{ij} on the ground motion attenuation. They modeled these two uncertainty terms as statistically independent normal random variates with zero mean values. The standard deviations of these two normal variates (say, τ and σ respectively, for η_i and ε_{ij}) are found to have dependence on the magnitude of generating earthquakes (Abrahamson and Silva 1997). Recent research identified that in addition to earthquake magnitude, τ and σ also depend on soil nonlinearity (Abrahamson and Silva 2008). Closed-form empirical equations are proposed in this literature to represent the standard deviations τ and σ in terms of earthquake magnitude, mean PGA at rock, shear wave velocity at site, and spectral time period. However, no definite correlation between uncertainty terms and the abovementioned source and site parameters is found through which η_i and ε_{ij} can be quantified explicitly. Therefore, the proposed NGA models (including closed-form equations for uncertainty terms) may not provide accurate estimates of ground motion intensities at different locations in the distribution region.

Due to the inherent randomness of the ground motion distribution process, the present study proposes the use of simulation-based approach to model and analyze the aleatory uncertainties. Assuming these are independent variables, inter- and intra-event uncertainties are represented here with a Gaussian random variable and a two-dimensional stationary Gaussian random field, respectively. NGA relationships (only for calculating $\hat{Y}_{ij}$) and ground motion records from NGA database are used here. Ground motion intensity is measured in terms of PGA, although any other intensity parameter such as spectral accelerations at various periods can also be used for this purpose. To demonstrate the uncertainty simulation, an initial discussion on one of the NGA models and some relevant statistical analyses are necessary.

NGA MODEL BY ABRAHAMSON AND SILVA (2008) FOR MEDIAN GROUND MOTION INTENSITY

Abrahamson and Silva (2008) proposed the next generation attenuation (NGA) model to evaluate the median estimate of ground motion intensities (Eq. 2). This relationship is developed using 2754 recordings from 135 earthquakes.

$$\begin{aligned}\ln\left(\hat{Y}\right) = & f_1\left(M, R_{rup}\right) + a_{12}F_{RV} + a_{13}F_{NM} + a_{15}F_{AS} + F_{HW} f_4\left(M, R_{rup}, R_{jb}, R_x, W, \delta, Z_{TOR}\right) \\ & + f_5\left(PGA_{1100}, V_{S30}\right) + f_6\left(Z_{TOR}\right) + f_8\left(R_{rup}, M\right) + f_{10}\left(Z_{1.0}, V_{S30}\right) \qquad (2)\end{aligned}$$

Here $\hat{Y}$ represents the median value of ground motion intensity. f_1 represents the base model which is a function of earthquake magnitude (M) and rupture distance (R_{rup}). R_{rup} is a measure of distance between source and site. F_{RV}, F_{NM}, F_{AS}, and F_{HW} are factors respectively representing the effects of reverse faulting earthquake, normal faulting earthquake, after shock and hanging wall on the ground motion attenuation. f_4 is associated with the hanging wall model which is a function of M, R_{rup}, Joyner-Boore distance (R_{jb}), horizontal distance from top edge to rupture (R_x), width of down-dip rupture (W), fault dip (δ), and depth-to-top of rupture (Z_{TOR}). The site response model is expressed with f_5 that represents the nonlinearity in site soil condition as a function of site shear wave velocity over the top 30 m (V_{S30}) and pick ground acceleration for rock sites (PGA_{1100}; in this case V_{S30} = 1100 m/s). f_6, f_8 and f_{10} respectively represent depth-to-top of rupture model, large distance model and soil depth model where $Z_{1.0}$ corresponds to the depth to shear wave velocity = 1.0 km/s. a_{12}, a_{13}, and a_{15} are various model coefficients.

In the present study, 487 records of ground motion intensities from 10 different California earthquakes are taken from NGA database (Table 1). These data are selected based on the following criteria:

(i) All records are from main shocks.
(ii) Recording sites exclude handing walls; this criterion is made to avoid statistical uncertainty due to limited available data on hanging walls.
(iii) Any record beyond 100 km from the source is ignored; this is considered based on the fact that beyond 100 km ground motion intensities attenuate to a great extent which can be ignored for the risk assessment of regional infrastructures.
(iv) V_{S30} is always considered to be less than V_{LIN} (V_{LIN} is defined as a shear-wave velocity below which site response is nonlinear; Abrahamson and Silva 2008); this is to study the effect of soil nonlianearity on the attenuation relation.

These four criteria yield F_{AS}, F_{HW} and f_8 equal to zero. In addition, the influence of f_{10} on the ground motion attenuation is not studied here primarily for two reasons; (*i*) very limited data on $Z_{1.0}$ is found in NGA database for some of the earthquakes that are considered in this study (e.g., Coalinga, Landers, Hector Mine and North Palm Spring) and (*ii*) soil depth (i.e., shallow or deep) is found to have no effect on median PGA (Abrahamson and Silva 2008).

Table 1: Selected earthquakes from NGA database (in alphabetic order)

Earthquake	Year of Occurrence	NGA ID	Magnitude	Fault Mechanism	Z_{TOR} (km)	# of recordings
Coalinga	1983	76	6.36	Reverse	3.4	31
Hector Mine	1999	158	7.13	Strike-slip	0	29
Imperial Valley	1979	50	6.53	Strike-slip	0	33
Landers	1992	125	7.28	Strike-slip	0	21
Loma Prieta	1989	118	6.93	Reverse-oblique	3.8	69
Morgan Hill	1984	90	6.19	Strike-slip	0.5	27
N Palm Springs	1986	101	6.06	Reverse-oblique	4	28
Northridge	1994	127	6.69	Reverse	5	132
San Fernando	1971	30	6.61	Reverse	0	22
Whittier Narrows	1987	113	5.99	Reverse-oblique	14.5	95

Incorporating these selection criteria, Eq. (2) takes the form of Eq. (3). Different components of this equation are described in following paragraphs.

$$\ln\left(\hat{Y}\right) = f_1\left(M, R_{rup}\right) + a_{12}F_{RV} + a_{13}F_{NM} + f_5\left(PGA_{1100}, V_{S30}\right) + f_6\left(Z_{TOR}\right) \tag{3}$$

Component 1 - Base model (f_1): The base model exhibits a gradual attenuation of ground motion intensity with distance from earthquake source. This is given as

$$f_1\left(M, R_{rup}\right) = \begin{cases} a_1 + a_4\left(M - c_1\right) + a_8\left(8.5 - M\right)^2 + \left[a_2 + a_3\left(M - c_1\right)\right]\ln\left(R\right) & \text{for } M \le c_1 \\ a_1 + a_5\left(M - c_1\right) + a_8\left(8.5 - M\right)^2 + \left[a_2 + a_3\left(M - c_1\right)\right]\ln\left(R\right) & \text{for } M > c_1 \end{cases} \tag{4}$$

where $R=\sqrt{R_{rup}^2+c_4^2}$. Values of a_1, a_4, a_5, a_8, c_1 and c_4 can be obtained from Abrahamson and Silva (2008).

Component 2 - Effect of faulting (F_{RV} and F_{NM}): Depending on the source mechanism, F_{RV} and F_{NM} can be determined as 1 or 0.

Component 3 - Site response model: This model represents site characteristics. In NGA database, five different soil types namely A, B, C, D, and E are identified based on preferred V_{S30}. Two extreme soil types, class A and E respectively represent hard rock (V_{S30} > 1500 m/s) and soft clay (V_{S30} < 180m/s), and other three types fall in between. 487 earthquake records used in this study have V_{S30} ranging from 116.4 m/s to 813.5 m/s and V_{LIN} for PGA is considered to be 865.1 m/s as reported in Abrahamson and Silva (2008). This indicates that for all 10 earthquakes used here, selected recordings are associated with nonlinear site response (as $V_{S30} < V_{LIN}$).

Site response model can be written as (proposed by Abrahamson and Silva 2008)

$$f_5(PGA_{1100},V_{S30})=\begin{cases} a_{10}\ln\left(\dfrac{V_{S30}}{V_{LIN}}\right)-b\ln(PGA_{1100}+c) & \\ \quad +b\ln\left(PGA_{1100}+c\left(\dfrac{V_{S30}}{V_{LIN}}\right)^n\right) & \text{for } V_{S30}<V_{LIN} \\ (a_{10}+bn)\ln\left(\dfrac{V_{S30}}{V_{LIN}}\right) & \text{for } V_{LIN}\le V_{S30}<V_1 \end{cases} \tag{5}$$

Values of a_{10}, b, c, and n are obtainable for the literature and V_1 = 1500 m/s for PGA.

Component 4 - Depth-to-top of rupture model (f_6): This model is expressed in the form of Eq. (6) where the value of a_{16} is given in Abrahamson and Silva (2008).

$$f_6(Z_{TOR})=\begin{cases} \dfrac{a_{16}Z_{TOR}}{10} & \text{for } Z_{\mathrm{TOR}}<10\,\text{km} \\ a_{16} & \text{for } Z_{\mathrm{TOR}}\ge 10\,\text{km} \end{cases} \tag{6}$$

Among these four components of Eq. (3), 1, 2 and 4 are introduced to account for the effects of source characteristics and source-to-site distance (i.e., rupture distance R_{rup}). Therefore, summation of these three components will provide a gradual attenuation of PGA from seismic source with increasing R_{rup}. Component 3 introduces nonlinearity in the attenuation model when $V_{S30} < V_{LIN}$. This is the case of the present study.

In order to evaluate median PGA ($\mathrm{PGA_{median}}$) over the entire distribution region, PGA_{1100} needs to be calculated first. This is done by applying V_{S30} = 1100 m/s in Eq. (3) which resulted in the following expression of PGA_{1100}.

$$\ln(PGA_{1100})=f_1(M,R_{rup})+a_{12}F_{RV}+a_{13}F_{NM}+f_5(V_{S30}=1100)+f_6(Z_{TOR}) \tag{7}$$

Figure 1 shows the variation of PGA_{median} and PGA_{1100} for two of the earthquakes, Northridge and Loma Prieta, considered herein. This also shows the recoded PGA values (with red open circles) at different recording stations for these two earthquakes. Note that PGA_{1100} has gradual attenuation while PGA_{median} is random. This is due to the fact that f_5 becomes linear for PGA_{1100} (i.e., for V_{S30} = 1100 m/s). Similar trends are observed for other earthquake ground motions as well.

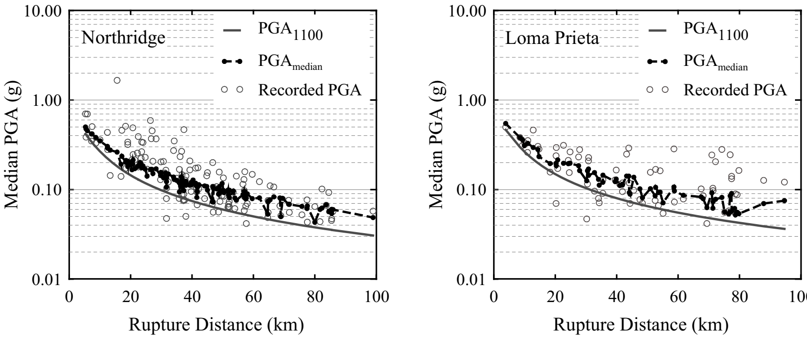

Figure 1. Attenuation of median ground motion intensity

SIMULATION OF NONLINEAR SITE RESPONSE

Uncertainties associated with the current attenuation model can be easily visualized from Figure 1. Besides, the distribution of median PGA (PGA_{median}) is random in nature when the site response is nonlinear (i.e., f_5 is nonlinear). Therefore, utilizing the attenuation relationship described in the preceding section, one cannot estimate the attenuation of PGA_{median} of any scenario earthquake using only information related to source characteristics and source-to-site distance. Distribution of V_{S30} over the entire region is also necessary for this purpose.

In NGA database, information on V_{S30} is available only at the recording stations. For any other sites, V_{S30} must be predicted from that recorded at nearby recording stations. Figure 1 shows random trends of the variation of V_{S30} between any two consecutive recordings. Therefore, the method of interpolation may not provide accurate information of V_{S30} at any arbitrary site other than recording stations. This complexity makes it difficult to estimate median PGA at sites where V_{S30} is not readily available. To overcome this difficulty, the current study assigns a suitable probabilistic distribution for the nonlinear site response. First, 487 values of f_5 from 487 records of 10 earthquakes are calculated. These f_5 values correspond to nonlinear site response according to forth ground motion selection criteria. Figure 2 represents the histogram of 487 values of f_5. A goodness-of-fit test is performed that resulted in a normal distribution at levels of significance of 0.01 and 0.05. The mean and standard deviation of the normal distribution are estimated to be 0.3002 and 0.1296, respectively. This distribution of f_5 is used to simulate the values of median PGA. Figure 3 represents the calculated PGA_{median} and its simulated values (in blue circles) for Northridge earthquake. Comparison shows good agreement between them.

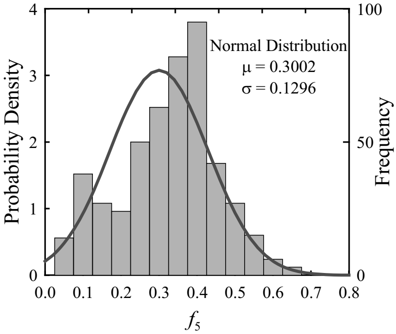

Figure 2. Histogram of 487 values of f_5 and the best-fitted probability distribution

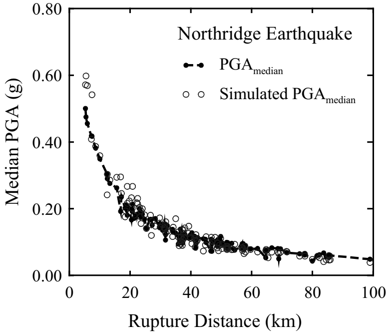

Figure 3. Calculated and simulated PGA_{median} at recording stations

MODELING OF INTER- AND INTRA-EVENT UNCERTAINTY

Modeling of Inter-event Uncertainty: Inter-event uncertainty (η_i) represents the random effect of i^{th} event. This is modeled as a Gaussion random variable with zero mean and standard deviation τ. Therefore the expression becomes, $\eta_i = N(0,\tau)$.

Modeling of Intra-event Uncertainty: The random effect of j^{th} recording of the i^{th} event is represented by intra-event uncertainty (ε_{ij}). A two-dimensional (2D) stationary Gaussian random field with standard deviation σ is considered to model the uncertainty. A region of 40 km × 40 km is chosen to be the distributed region of the ground motion. The upper cut-off wave number is set to 5 rad/km. Simulation results are discussed in the following section.

SIMULATION RESULTS AND DISCUSSIONS

Two sets of simulations are performed for all 10 earthquakes; (i) Case I with $\tau = \sigma = 0.2$ and (ii) Case II with $\tau = 1.0$ and $\sigma = 0.2$. Figure 4 and 5 show the simulation results obtained in Case I and Case II, respectively for Northridge earthquake. Each figure consists of four plots showing the simulation of median PGA (a) without uncertainty, (b) with inter-event uncertainty, (c) with intra-event uncertainty, and (d) with both uncertainties. All of these plots show randomness of ground motion distribution. The randomness in plot (a) is purely due to the random nature of nonlinear site response, while the same is due to the combined effect of nonlinear site response and aleatory uncertainty (either inter-event or intra-event or both) in other three plots.

In Case I (Figure 4), difference between (a) and (b) is trivial, whereas the same in Case II is significant (Figure 5). This is due to assigned values of standard deviations of inter-event uncertainty (τ). Lower τ does not insert much variation in the ground motion attenuation relationship. In all cases, the effect of inter-event uncertainty remains constant for one simulation and does not changes spatially.